Title

Kcne4 deletion sex- and age-specifically impairs cardiac repolarization in mice.

Journal

FASEB journal : official publication of the Federation of American Societies for Experimental Biology, 30(1)

ISSN

0892-6638

Authors

Crump, Shawn M
Hu, Zhaoyang
Kant, Ritu
et al.

Publication Date

2016

DOI

10.1096/fj.15-278754

Kcne4 deletion sex- and age-specifically impairs cardiac repolarization in mice

Shawn M. Crump,*[,1] Zhaoyang Hu,[†,1] Ritu Kant,* Daniel I. Levy,[‡,2] Steve A. N. Goldstein,[§] and Geoffrey W. Abbott*[,3]

*Bioelectricity Laboratory, Department of Pharmacology and Department of Physiology and Biophysics, School of Medicine, University of California, Irvine, Irvine, California, USA; [†]Department of Anesthesiology and Translational Neuroscience Center, West China Hospital, Sichuan University, Chengdu, People's Republic of China; [‡]Section of Nephrology, Department of Medicine, University of Chicago, Chicago, Illinois, USA; and [§]Department of Biochemistry, Brandeis University, Waltham, Massachusetts, USA

ABSTRACT **Myocardial repolarization capacity varies with sex, age, and pathology; the molecular basis for this variation is incompletely understood. Here, we show that the transcript for KCNE4, a voltage-gated potassium (K_v) channel β subunit associated with human atrial fibrillation, was 8-fold more highly expressed in the male left ventricle compared with females in young adult C57BL/6 mice ($P < 0.05$). Similarly, K_v current density was 25% greater in ventricular myocytes from young adult males ($P < 0.05$). Germ-line *Kcne4* deletion eliminated the sex-specific K_v current disparity by diminishing ventricular fast transient outward current ($I_{to,f}$) and slowly activating K^+ current ($I_{K,slow1}$). *Kcne4* deletion also reduced K_v currents in male mouse atrial myocytes, by >45% ($P < 0.001$). As we previously found for $K_v4.2$ (which generates mouse $I_{to,f}$), heterologously expressed KCNE4 functionally regulated $K_v1.5$ (the K_v α subunit that generates I_{Kslow1} in mice). Of note, in postmenopausal female mice, ventricular repolarization was impaired by *Kcne4* deletion, and ventricular *Kcne4* expression increased to match that of males. Moreover, castration diminished male ventricular *Kcne4* expression 2.8-fold, whereas 5α-dihydrotestosterone (DHT) implants in castrated mice increased Kcne4 expression >3-fold ($P = 0.01$) to match noncastrated levels. KCNE4 is thereby shown to be a DHT-regulated determinant of cardiac excitability and a molecular substrate for sex- and age-dependent cardiac arrhythmogenesis.—Crump, S. M., Hu, Z., Kant, R., Levy, D. I., Goldstein, S. A. N., Abbott, G. W. *Kcne4* deletion sex- and age-specifically impairs cardiac repolarization in mice. *FASEB J.* 30, 360–369 (2016). www.fasebj.org**

Cardiac myocyte repolarization is a complex process requiring the concerted action of several different types of potassium channel (1). Voltage-gated potassium (K_v) channels comprise both pore-forming α subunits and regulatory proteins including β subunits such as the single-pass transmembrane KCNE proteins (2) (**Fig. 1*A***).

In human ventricular myocardium, the delayed rectifier currents I_{Kr} and I_{Ks} are the primary repolarizing currents. Generated by hERG and KCNQ1 K_v α subunits, respectively, these K^+ currents repolarize ventricular myocytes after a plateau phase lasting several hundred milliseconds (1). In adult mouse ventricles, ventricular myocyte action potentials are much shorter; I_{Kr} is absent, and I_{Ks} is, at most, weakly expressed and detectable only after β-adrenergic stimulation (3). Instead, the rapidly activating and inactivating I_{to} and the rapidly activating, slowly inactivating K^+ current ($I_{K,slow}$) dominate adult mouse ventricular repolarization (4).

It is noteworthy that various members of the KCNE family, of which there are 5 members in mammals, are expressed in both human and mouse heart. The KCNE proteins can each form complexes with 1 or more K_v α subunits, generating heteromeric channel assemblies often with unique gating or other functional properties (2). KCNE subunits can also regulate α subunit trafficking and subcellular localization (5). Although human and mouse hearts exhibit fundamental differences in the K^+ currents that shape their action potentials, previous studies have demonstrated that the same KCNE isoforms can be influential in myocardial repolarization of either species—at least partly because of their functional versatility (6, 7). *KCNE* gene variants are linked to human cardiac arrhythmias including Long QT syndrome, atrial fibrillation (AF), and Brugada syndrome; *Kcne* gene deletion in mice can cause analogous pathologies (8).

Abbreviations: 4-AP, 4-aminopyridine; AF, atrial fibrillation; ARE, androgen-responsive element; BSA, bovine serum albumin; CFP, cyan fluorescent protein; CHO, Chinese hamster ovary; co-IP, coimmunoprecipitation; DHT, 5α-dihydrotestosterone; HEPES, 4-(2-hydroxyethyl)piperazine-1-ethanesulfonic acid; IF, immunofluorescence; $I_{K,slow}$, slowly activating K^+ current;

(*continued on next page*)

[1] These authors contributed equally to this work.

[2] Current affiliation: Global Innovative Pharma, Pfizer Inc., Collegeville, PA, USA.

[3] Correspondence: A-360 Medical Surge II, Department of Pharmacology, School of Medicine, University of California, Irvine, Irvine, CA 92697-4625, USA. E-mail: abbottg@uci.edu

doi: 10.1096/fj.15-278754

This article includes supplemental data. Please visit *http://www.fasebj.org* to obtain this information.

0892-6638/16/0030-0360 © FASEB

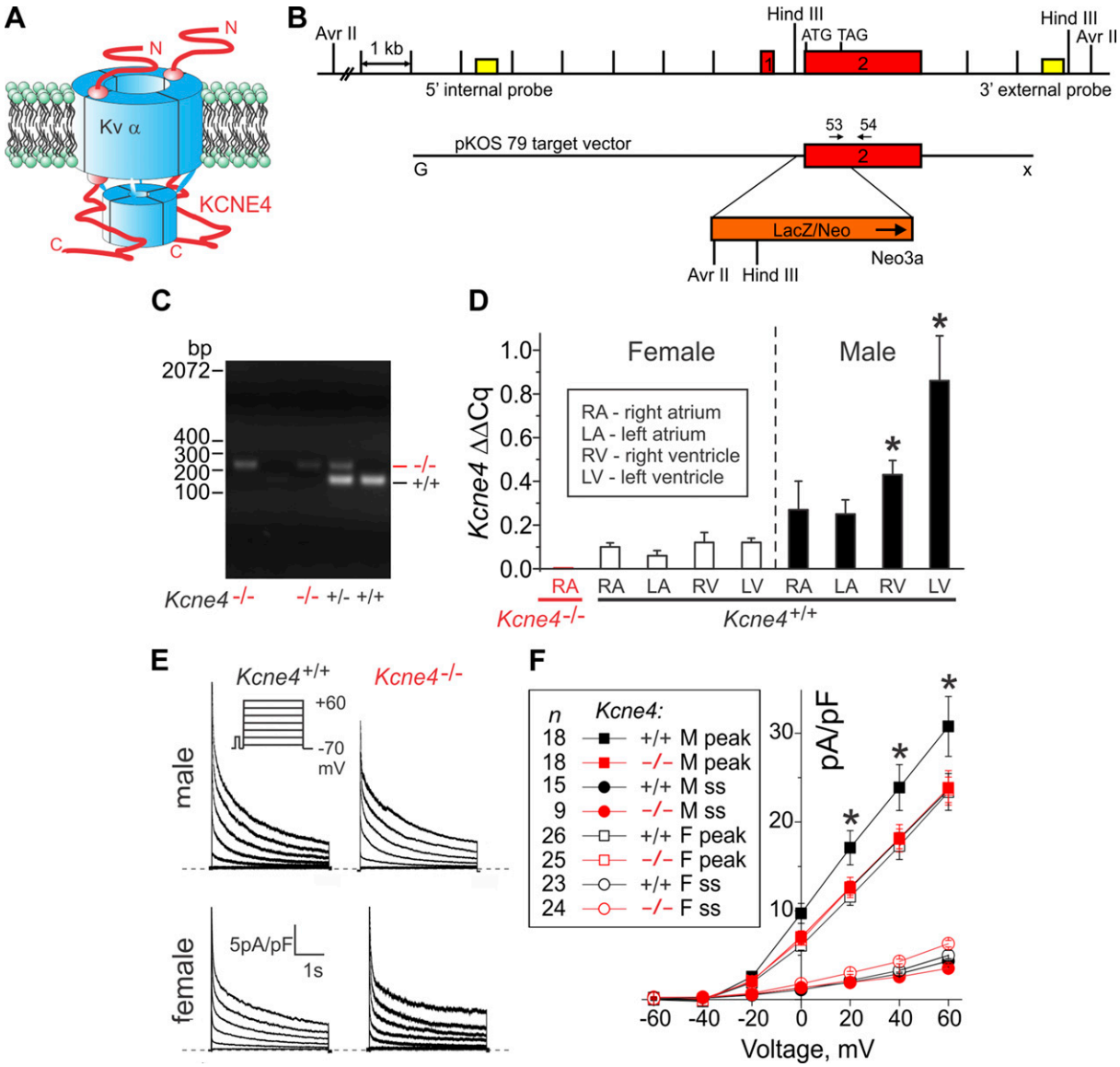

Figure 1. *Kcne4* deletion sex-specifically impairs mouse ventricular myocyte K^+ currents. *A*) Cartoon of KCNE4 subunits in a $K_v\alpha$-KCNE4 channel complex, with a hypothetical 4:2 stoichiometry. *B*) Strategy for germ-line *Kcne4* deletion from mice (Materials and Methods). *C*) Genotyping gel of PCR of genomic DNA extracted from tail tip tissue confirming *Kcne4* deletion from mice. *D*) Relative *Kcne4* expression by real-time qPCR quantification of sexually mature adult (6 mo old) mouse heart chambers. $*P < 0.05$ compared with corresponding female ventricles. All values were normalized to one of the 4- to 6-mo-old male $Kcne4^{+/+}$ mouse LV *Kcne4* expression values. *E*) Representative whole-cell ventricular septal cardiomyocyte K^+ currents from male and female sexually mature adult (10 mo old) $Kcne4^{+/+}$ and $Kcne4^{-/-}$ mice (voltage protocol inset); $n = 9$–26 myocytes from 3 to 6 mice per group. *F*) Mean peak and steady-state whole-cell ventricular septal cardiomyocyte K^+ current densities recorded from cells as in *C*, isolated from male (M) or female (F) mice; genotypes are as shown. $*P < 0.05$ compared with other peak currents at equivalent voltages; $n = 9$–26 cells per group, as indicated.

An important issue in human cardiac arrhythmia is the variable penetrance of disease between individuals harboring the same gene variant. One of the more important sources of variability is the sex of the individual (9). Brugada syndrome, most commonly linked to loss-of-function SCN5A variants, is 8-fold more common in men than women (10). Reduced repolarization reserve and lower I_{Kr} density are more commonly observed in women than in men and predispose to drug-induced cardiac arrhythmia (9). Uncovering sex-dependent differences in arrhythmia susceptibility and the molecular mechanisms underlying them is therefore an early step toward therapeutic strategies tailored toward the individual (*i.e.*, precision medicine) (11).

KCNE4, which we originally named MinK-related peptide 3 (6), functionally regulates KCNQ1, $K_v1.1$, $K_v1.3$, $K_v4.2$, $K_v4.3$, and the Ca^{2+}-activated K^+ channel, in heterologous coexpression experiments (12–18). A

(*continued from previous page*)

$I_{to,f}$, fast transient outward current; $I_{to,s}$, slow transient outward current; K_v, voltage-gated potassium; qPCR, quantitative PCR; QT_c, corrected QT interval; ss, steady state; TEA, tetraethylammonium

single nucleotide polymorphism generating an E145D substitution, positioned in the atypically lengthy cytoplasmic C-terminal end of KCNE4, is an independent risk factor for AF in Han (in 3 separate analyses) and Uygur Chinese (19–21). KCNE4 inhibits KCNQ1 activity, but E145D-KCNE4 augments KCNQ1 current, suggesting a potential mechanistic basis for E145D-associated AF (22). Here, we examined the effects of targeted *Kcne4* gene deletion in mice and discovered sex-dependent differences in expression and function that were explained by 5α-dihydrotestosterone (DHT) regulation of cardiac KCNE4 expression.

MATERIALS AND METHODS

Kcne4$^{-/-}$ mice

Mice were housed in a pathogen-free facility. The present study was approved by the Animal Care and Use Committees at University of California, Irvine and carried out in accordance with the recommendations in the *Guide for the Care and Use of Laboratory Animals* (National Institutes of Health, Bethesda, MD, USA). C57BL/6 *Kcne4*$^{-/-}$ mice were generated by replacement of the sole coding exon of *Kcne4* with neo and *LacZ* genes (Fig. 1*B*) in 129/Sv embryonic stem cells for embryonic injection followed by implantation into a C57 breeder, PCR screening of progeny, and confirmed Southern blot analysis (performed by Lexicon, The Woodlands, TX, USA; and Texas A&M Institute for Genomic Medicine, College Station, TX, USA; data not shown). *Kcne4*$^{+/-}$ mice were then backcrossed for at least 10 generations into the C57BL/6 strain. Colony genotyping was performed by conventional PCR of genomic DNA isolated from tail tip tissue (Fig. 1*C*). The PCR primer sequences were as follows: *Kcne4* forward 5′-CAACGACAGCAGTGAAGGC-3′, *Kcne4* reverse 5′-GCAGAGCAAAAGCAAAACCC-3′, Neo3a 5′-GCAGCGCATCGCCTTCTATC-3′; *Kcne4*$^{+/+}$ band, 137 bp, *Kcne4*$^{-/-}$ band, 229 bp. Castration and DHT pellet implants (7.5 mg DHT, 90-d release; Innovative Research of America, Sarasota, FL, USA) were performed by Charles River Laboratories (Hollister, CA, USA).

Real-time quantitative PCR

Mice were killed by CO_2 asphyxiation. Hearts were quickly harvested, washed, and perfused through the left ventricle with PBS + heparin and then processed or stored at −80°C until use. RNA was extracted using 1 ml Trizol (Invitrogen, Carlsbad, CA, USA)/100 mg tissue and purified using the RNeasy Mini Kit (Qiagen, Valencia, CA, USA) according to the manufacturers' protocol. RNA samples with A_{260}/A_{280} absorbance ratios between 2.00 and 2.20 were used for further synthesis; 500 ng to 1 μg RNA was used for cDNA synthesis (Quantitect Reverse Transcriptase; Qiagen) and stored at −20°C until use. Primer pairs for target genes *Kcne4* (NCBI Gene ID 57814) and *GAPDH* (NCBI Gene ID: 14433) produced an amplicon of 137 and 123 bp, respectively. Primer sequences were obtained from MGH-ParaBioSys:NHLBI Program for Genomic Applications, Massachusetts General Hospital, and Harvard Medical School (Boston, MA, USA) (http://pga.mgh.harvard.edu). The sequences of primers (0.05 μm scale, HPLC purified; Sigma-Aldrich, St. Louis, MO, USA) were as follows: *Kcne4*, forward 5′-CTTTGCTCGATGGAAGGGGAC-3′, reverse 5′-GCTGTCGTTGAGAGGCGTC-3′; *Gapdh*, forward 5′-AGGTCGGTGTGAACGGATTTG-3′, reverse 5′-TGTAGACCATGTAGTTGAGGTCA-3′. Real-time quantitative PCR (qPCR) analysis was performed using the CFX Connect System, iTaq Universal SYBR Green Supermix (Bio-Rad, Hercules, CA, USA) and 96-well clear plates. Thermocycling parameters were set according to the manufacturer's protocol for iTaq. Samples were run in triplicate as a quality control measure, and triplicates with an SD of 0.600 or higher were repeated. Melting curves were assessed for verification of a single product. Final analysis measuring statistical significance was calculated measuring $\Delta\Delta C_q$ values normalized to the 6-mo-old male *Kcne4*$^{+/+}$ left ventricle data.

Antibodies

Chicken and rabbit antibodies were generated to human KCNE4 residues 67–138 for Western blot/coimmunoprecipitation (co-IP) and residues 136–150 for immunofluorescence (IF), respectively, as described previously (18). Commercial voltage-gated K^+ channel antibodies raised against rabbit anti-K_v1.5 (Alomone Laboratories, Jerusalem, Israel) were used for Western blots and IF as described previously (7, 23).

Isolation of adult mouse cardiomyocytes

Single cardiomyocytes were isolated from sexually mature adult (10 mo old) mice that were heparinized using (250 IU, i.p., to minimize blood clotting) for 10 min before CO_2 gas and cervical dislocation. The chest was opened to expose the heart and lungs. Hearts were quickly excised, and cannulation of ascending aorta was perfused on a 37°C warmed Langendorff apparatus (Easy Cell Extraction System Type 803; Hugo Sacks Elektronik, March-Hugstetten, Germany) constantly gassed with 95% O_2–5% CO_2. The hearts were perfused at 3 ml/min with calcium-free 4-(2-hydroxyethyl) piperazine-1-ethanesulfonic acid (HEPES) buffer containing the following (in mM): 137 NaCl, 5.4 KCl, 1.2 $MgSO_4$, 15 NaH_2PO_4, 20 glucose, 10 HEPES, and 2 L-glutamine (pH 7.4, buffer A) for 5 min, followed by 10–14 min of 0.36 mg/ml type II collagenase (Worthington, Lakewood, NJ, USA) and 10 μM $CaCl_2$ (buffer B) or until the hearts were swollen and pale in color. The hearts were transferred to a 10 cm dish containing buffer A supplemented with 5 mg/ml bovine serum albumin (BSA) and 150 μM $CaCl_2$ (buffer C) and mechanically dissociated using forceps until large pieces were dispersed into the cells suspension. Undigested tissue debris were filtered through a 200 μM nylon mesh into a Falcon tube, and 2 volumes of buffer A supplemented with 5 mg/ml BSA and 1 mM $CaCl_2$ solution (buffer D) were added and allowed to settle for 5 min. Cells were rinsed and pelleted 2 times at 300 rpm for 3 min and resuspended in buffer D. Cells were resuspended to desired cell concentration using buffer D for electrophysiology or seeded on laminin (Corning, Tewksbury, MA, USA)-coated glass coverslips (15 μg/ml) for IF assay. Only rod-shaped cardiomyocytes with clear striations were used for recording.

Cellular electrophysiology

Whole-cell patch-clamp recordings from dispersed adult cardiomyocytes or transfected Chinese hamster ovary (CHO) cells were performed at room temperature using an IX50 inverted microscope equipped with an FHD chamber from IonOptix (Olympus, Center Valley, PA, USA), a Multiclamp 700A Amplifier, a Digidata 1300 Analog/Digital converter, and PC with pClamp9 software (Molecular Devices, Sunnyvale, CA, USA). For cardiomyocytes, the bath solution contained the following (in mM): 117 NaCl, 4 KCl, 1.7 $MgCl_2$, 10 HEPES, 1 KH_2PO_4, 4 $NaHCO_3$, 3 $CoCl_2$, and 10 D-glucose (pH 7.4 with NaOH).

Pipettes were of 2.1–3.2 MΩ resistance when filled with intracellular solution containing the following (in mM): 130 KCl, 2 $MgCl_2$, 20 HEPES, 11 EGTA, 5 Na_2ATP, 0.4 Na_2GTP, and 5 Na_2CP (pH 7.4 with KOH). Outward K^+ currents were evoked during 4.5 second voltage steps to test potentials between –60 and +60 mV in 20 mV increments from a holding potential of –70 mV after a 100 ms prepulse to –40 mV. Leak currents were always <100 pA and were not corrected. Data were analyzed using pClamp9.1 software (Molecular Devices, Sunnyvale, CA, USA), and statistical analysis (ANOVA) was performed using Origin 6.1 (Microcal, Northampton, MA, USA) software. The decay phase of I_K was fitted to the sum of 3 exponentials to quantify the τ of decay and current amplitude for $I_{K,slow}$, fast transient outward current ($I_{to,f}$), and slow transient outward current ($I_{to,s}$) as before (7).

For inhibition of $K_v1.5$ and $K_v2.1$, respectively, 50 μM 4-aminopyridine (4-AP; ICN Biomedicals, Irvine, CA, USA) and 25 mM tetraethylammonium (TEA; Sigma-Aldrich) bath solutions were applied to the recording bath to achieve at least 4× bulk flow bath displacement after baseline recordings and allowed to equilibrate for 2–3 min before drug recordings.

For whole-cell patch clamp of CHO cells, bath solution contained the following (in mM): 135 NaCl, 5 KCl, 1.2 $MgCl_2$, 5 HEPES, 2.5 $CaCl_2$, and 10 D-glucose (pH 7.4). Pipettes were 2.1–3.5 MΩ resistance when filled with intracellular solution containing the following (in mM): 10 NaCl, 117 KCl, 2 $MgCl_2$, 11 HEPES, 11 EGTA, and 1 $CaCl_2$ (pH 7.2). K^+ currents were evoked during a 1 second voltage step in 10 mV increments between −80 and +60 mV from a holding potential of −75 mV. Green fluorescent protein-positive cells were selected for recording 24 h after transfection.

For all current and current density comparisons, currents between 0 and 50 or 60 mV were compared between genotypes, with ANOVA followed by Bonferroni correction for multiple comparisons to determine *P* values.

Cell culture and transfection

CHO cells were cultured at 37°C and 5% CO_2 in F12K medium (ATCC, Manassas, VA, USA) containing L-glutamine and sodium bicarbonate supplemented with 10% fetal bovine serum (Invitrogen) plus 1% penicillin and streptomycin. CHO cells were cultured in 10 cm tissue culture plates to 80% confluence. Next, CHO cells were washed once with PBS (Ca^{2+} and Mg^{2+} free; Invitrogen) and then incubated with Detachin (Genlantis, San Diego, CA, USA) for 3 min. Fetal bovine serum–supplemented F12K medium was added, and cells were centrifuged for 2 min at 1000 rpm. For transfection, 2×10^5 cells were seeded in 35 mm tissue culture dishes 2 h before transfection. CHO medium was replaced with prewarmed Opti-MEM reduced serum medium (Invitrogen) and transiently transfected using a 2:1 ratio of Lipofectamine 2000 (Invitrogen) to cDNA. Specifically for electrophysiology, cells were transfected with 0.02 μg human-$K_v1.5$ cDNA, 0.02 μg mouse-Kcne4 cDNA, 2.47 μg pBluescript (cells transfected without Kcne4 used 2.49 μg pBluescript), and 0.147 μg enhanced green fluorescent protein added (for identification of transfected cells) to 250 μl of Opti-MEM, followed by dropwise addition of Lipofectamine 2000 and incubated at room temperature for 20 min. Cell medium was replaced with fresh prewarmed 10% fetal bovine serum–supplemented F12K medium after 3 h of transfection. Whole-cell patch-clamp or IF experiments were conducted 24 h after transfection.

Immunofluorescence

CHO cells (4×10^5 cells per 10 cm dish) were transfected as described above and then rinsed twice in ice-cold PBS before fixation in ice-cold 4% paraformaldehyde for 10 min. All treatments for the rest of the procedure were at room temperature. Following fixation in formaldehyde, cells were permeated with PBS containing 0.25% Triton X-100 in 1% BSA for 10 min and then rinsed 3 times for 5 min with PBS. The cells were blocked with 1% BSA + 10% normal goat serum in PBS/0.25% Triton X-100 for 30 min. Blocking buffer was changed to primary antibody (1:200) and incubated for 3 h followed by 3 × 5 min PBS rinses. Cells were then incubated with secondary Fluor-antibodies (1:600) in 1% BSA/10% normal goat serum/PBS/0.25% Triton X-100 for 1 h. Cells were washed 3 × 5 min with PBS, and then the coverslips were mounted with DAPI-labeled mounting medium and visualized after drying using an Olympus BX51 microscope and CellSens software (Olympus, Waltham, MA, USA). Secondary antibodies used were donkey anti-chicken 488 and goat anti–rabbit-555 (Invitrogen). Effects of KCNE4 on $K_v1.5$ surface expression in live CHO cells were quantified using Nikon NIS Elements v4.10 software *via* a primary antibody raised against an extracellular epitope of $K_v1.5$ (APC-150; Alomone Laboratories); total cell $K_v1.5$ expression was quantified *via* a C-terminal cyan fluorescent protein (CFP) tag while maintaining the same time capture exposure for all images. In brief, a circular region of interest was overlaid and adjusted to the exact size of the CFP-$K_v1.5$ signal boundary to measure fluorescence. Next, the same circular region of interest pixel area and coordinates were used to measure the anti-$K_v1.5$ cell fluorescence in the same cell. Anti-$K_v1.5$ fluorescence was normalized to total $K_v1.5$-CFP fluorescence.

Western blot and co-IP

CHO cells were transiently transfected overnight with a 3:1 ratio of LT1 (Mirus, Madison, WI, USA) to cDNA in an 80% confluent 10 cm plate containing 2 μg human $K_v1.5$ + 2 μg mouse Kcne4 + 11 μg pBluescript. CHO cells were lysed 24 h after transfection after they were scraped, pelleted at 1000 rpm for 2 min, and then washed once in PBS. The cell pellet was lysed with 450 μl buffer containing 150 mM NaCl, 50 mM Tris, 1% Nonidet P-40, and 0.1% SDS (Sigma-Aldrich) with protease inhibitor (Thermo Fisher Scientific, Waltham, MA, USA), pH to 7.4, for 1 h at 4°C while rotating. Lysates were pelleted for 10 min at 10,000 rpm, and supernatant was collected for BCA protein quantification (Thermo Fisher Scientific) after preclearing with 40 μl of Pierce agarose A beads (Thermo Fisher Scientific). For Western blot analysis, 15 μg lysate per lane was fractionated by SDS-PAGE, transferred onto PVDF membranes, and probed with anti-Kcne4 or anti-$K_v1.5$ antibody, followed by horseradish peroxidase–conjugated goat anti-rabbit IgG secondary antibody (Bio-Rad) or goat anti-chicken IgY secondary antibody (Aves Laboratories, Tigard, OR, USA) for visualization with fluorography (ECL-plus; Amersham Biosciences/GE Healthcare Life Sciences, Marlborough, MA, USA). For co-IPs, 350 μg lysates was incubated overnight with primary antibody at 4°C, and then 40 μl of Pierce agarose A beads was added for 1 h. Beads were washed 3 × 5 min with lysis buffer and eluted with Tris (2-carboxyethyl)phosphine hydrochloride and NuPage LDS loading buffer (Novex Life Technologies, Carlsbad, CA, USA) at 95°C for 5 min. Elutions (20 μl/lane) were fractionated by SDS-PAGE as above for Western blotting. Blots were visualized using SynGene G:Box Chemi XR5, running Genesys software, v1.4.3 (Syngene, Frederick, MD, USA).

Electrocardiography and hemodynamic analyses

Mice in 3 age groups (4, 12, and 17 mo old) were anesthetized with 2% isoflurane, and surgical anesthesia was verified by a lack of response to toe pinch. The standard limb lead II configuration

electrocardiographic system was inserted subcutaneously to limbs by needle electrodes, and electrocardiograms were recorded throughout the study. QT, RR, PR, and QRS intervals and heart rate were analyzed offline after acquisition. Corrected QT interval (QT_c) was calculated based on Mitchell's formula specifically for mice (24): $QT_c = QT/(RR/100)^{1/2}$. For hemodynamic analysis, the right carotid artery was exposed through a cervical midline incision, and the left ventricle was catheterized *via* the right carotid artery using a 1.0 F Millar Micro-Tip catheter transducer (model SPR-1000) connected to a pressure transducer (Millar Instruments, Houston, TX, USA). Baseline blood pressures were recorded before advancing the catheter into the left ventricle. The real-time data were collected by Powerlab/8sp system (ADInstruments, Colorado Springs, CO, USA). LabChart 7.2.1 software (ADInstruments) was used for electrocardiographic and hemodynamic data acquisition and analysis.

RESULTS

Kcne4 transcript expression is enriched in ventricles of male sexually mature mice

We first quantified mouse cardiac *Kcne4* expression by real-time qPCR using *Kcne4*$^{-/-}$ tissue as a negative control and to further confirm genotype. In sexually mature mice, *Kcne4* expression was highest in the left ventricle of male mice, next highest in the male mouse right ventricle, and then the male atria, and was comparatively low in all 4 female heart chambers (Fig. 1*D*).

Kcne4 deletion sex-specifically impairs ventricular and atrial myocyte repolarization in mice

We next measured K_v currents using whole-cell patch clamp of ventricular myocytes isolated from sexually mature *Kcne4*$^{+/+}$ and *Kcne4*$^{-/-}$ mice. Mean current density (peak and sustained current) was unaffected by *Kcne4* deletion in female ventricular myocytes isolated from the septum (Fig. 1*E, F*) and also those from the apex (Supplemental Fig. S1). This was consistent with the relatively low expression of *Kcne4* in the female mouse heart. In contrast, *Kcne4* deletion reduced peak K_v current density in male ventricular septal myocytes to match that of females but did not alter sustained currents (Fig. 1*E, F*).

The 3 major components of adult mouse ventricular myocyte K_v currents ($I_{to,f}$, $I_{to,s}$, and $I_{K,slow}$) can be isolated by fitting current decay with 3 exponential functions, distinguishing their 3 different inactivation rates, and permitting quantification of the amplitude of each component (7, 25). The inactivation kinetics of the *Kcne4*-dependent current in males were consistent with it comprising both the rapidly inactivating $I_{to,f}$ (generated by K_v4 subunits in musine and human ventricles) and the more slowly inactivating $I_{K,slow}$ (generated by $K_v1.5$ and $K_v2.1$ α subunits in adult mouse ventricles), but not the intermediate-inactivating $I_{to,s}$ (generated by $K_v1.4$ in adult mouse ventricles) (**Fig. 2*A, B***). We previously demonstrated that KCNE4 augments $K_v4.2$ activity (17), consistent with the reduction in $I_{to,f}$ observed here on *Kcne4* deletion.

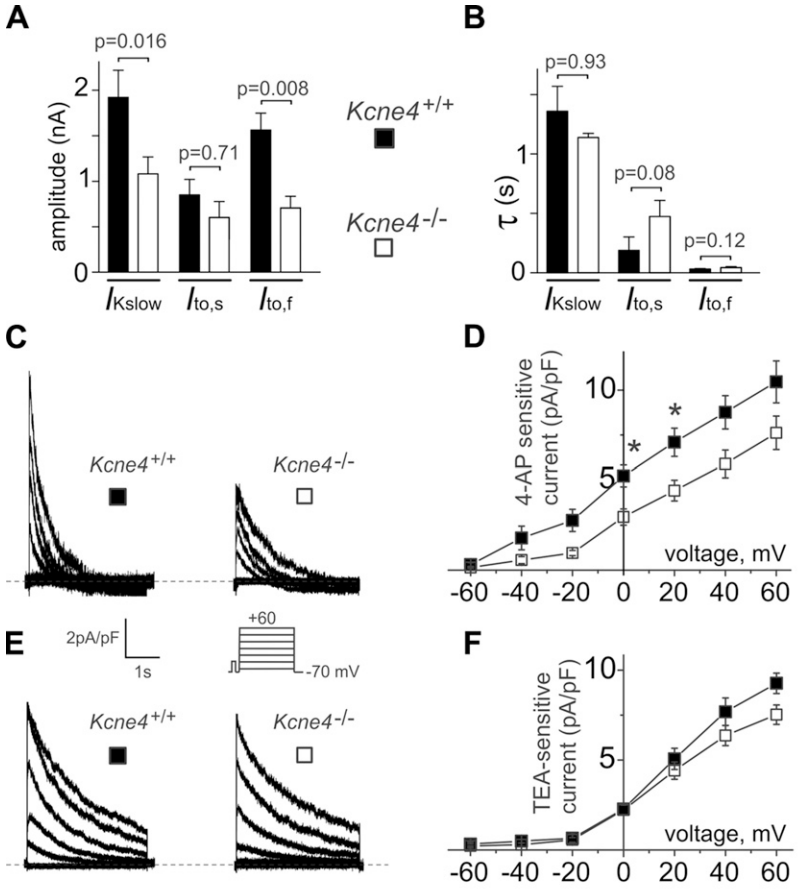

Figure 2. *Kcne4* deletion impairs male mouse ventricular myocyte $I_{to,f}$ and $I_{K,slow1}$. *A, B*) Mean amplitude (*A*) and decay time constant, τ (*B*), of current components after curve-fitting whole-cell ventricular septal cardiomyocyte K^+ current traces from male sexually mature adult *Kcne4*$^{+/+}$ and *Kcne4*$^{-/-}$ mice as in Fig. 1*E, F*; n = 9–26 myocytes from 3 to 6 mice per group. *C*) Exemplar digitally subtracted 50 μM 4-AP–sensitive K^+ current ($I_{K,slow1}$) traces recorded from cells as in Fig. 1*E, F*; genotypes are as shown; n = 18–19. *D*) Mean digitally subtracted 50 μM 4-AP–sensitive K^+ current ($I_{K,slow1}$) densities quantified from traces as in *C*; genotypes are as shown; n = 18–19. *$P < 0.01$ comparing current density between genotypes. *E*) Exemplar digitally subtracted 25 mM TEA-sensitive K^+ current ($I_{K,slow2}$) traces recorded from cells as in Fig. 1*E, F*; genotypes are as shown; n = 7–9. *F*) Mean digitally subtracted 25 mM TEA-sensitive K^+ current ($I_{K,slow2}$) densities quantified from traces as in *E*; genotypes are as shown; n = 7–9.

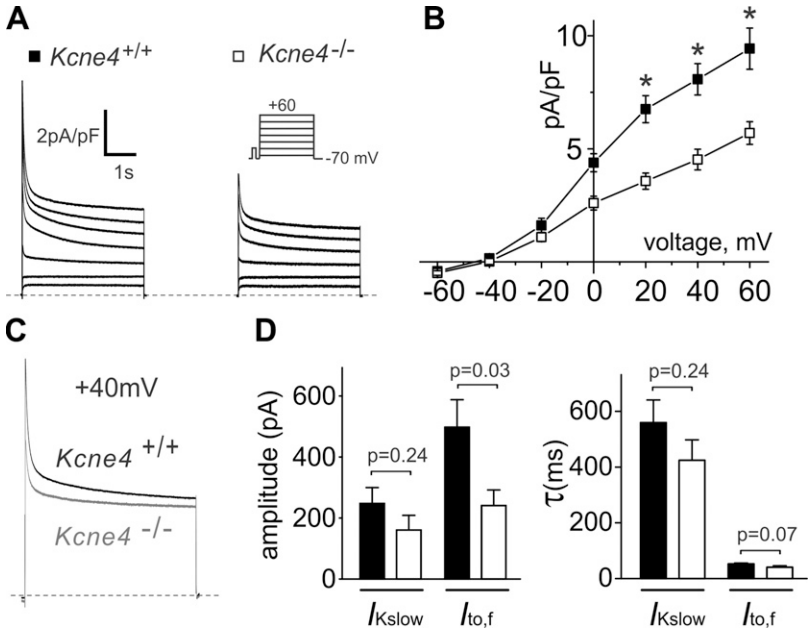

Figure 3. *Kcne4* deletion impairs male mouse atrial myocyte $I_{to,f}$. *A*) Representative whole-cell atrial cardiomyocyte K^+ currents from sexually mature adult male $Kcne4^{+/+}$ and $Kcne4^{-/-}$ mice (voltage protocol inset); $n = 20$ myocytes from 3 to 4 mice per group. *B*) Mean peak whole-cell atrial cardiomyocyte K^+ current densities recorded from cells as in *A*; $n = 20$, $^*P < 0.001$. *C*) Averaged K^+ current traces elicited by a +40 mV voltage pulse from atrial myocytes isolated from sexually mature adult male $Kcne4^{+/+}$ and $Kcne4^{-/-}$ mice (mean of 20 traces per genotype). *D*) Mean data resulting from curve fitting of +40 mV traces from recordings as in *A*; $n = 14$–19.

The ~50% loss of amplitude in $I_{K,slow}$ suggested a role for KCNE4 with $K_v1.5$ and/or $K_v2.1$ that had not been previously recognized. Indeed, pharmacologic isolation of the $I_{K,slow}$ component of the *Kcne4*-dependent current revealed its sensitivity to 50 μM 4-AP (Fig. 2*C, D*) but not 25 mM TEA (Fig. 2*E, F*). This profile was consistent with the pharmacologic properties of $I_{K,slow1}$, generated by $K_v1.5$ (7).

Kcne4 deletion also reduced K_v current density in adult male mouse atrial myocytes, by >45% at +40 mV ($P < 0.001$; **Fig. 3*A, B***). Curve fitting with 2 exponentials to isolate the rapid- and the slow-inactivating current components, as previously described for adult mouse atrial myocytes (26), revealed that the primary current component lost by *Kcne4* deletion was $I_{to,f}$ (>50% reduction at +40 mV; $P = 0.03$; Fig. 3*C, D*).

KCNE4 colocalizes with and augments activity of $K_v1.5$ in CHO cells

To validate the notion that KCNE4 directly regulates $K_v1.5$ channels, we studied the subunits heterologously expressed in CHO cells. KCNE4 more than doubled the density of current generated by $K_v1.5$ (**Fig. 4*A, B***). KCNE4 moderately increased the slope and left-shifted the voltage dependence of activation of $K_v1.5$ (Fig. 4*C*). KCNE4 did not alter activation kinetics but moderately increased the extent of inactivation over a 1 second pulse to +40 mV of $K_v1.5$ (Fig. 4*D, E*).

KCNE4 colocalized in the plasma membrane of CHO cells with coexpressed $K_v1.5$ (**Fig. 5*A***), and $K_v1.5$-KCNE4 complexes were detectable by co-IP (Fig. 5*B*). To quantify effects of KCNE4 on $K_v1.5$ surface expression, CFP-tagged $K_v1.5$ ($K_v1.5$-CFP) was expressed alone or with KCNE4 and CFP fluorescence compared with fluorescence from detection of antibody raised to an epitope on the surface of $K_v1.5$, using microscopy of live CHO cells. $K_v1.5$-CFP was expressed in puncta at the cell surface, and KCNE4 increased the number of puncta (Fig. 5*C*). Quantification of total and surface fluorescence intensities revealed that KCNE4 did not alter total $K_v1.5$-CFP expression but doubled $K_v1.5$-CFP surface expression, whether or not this value was normalized to total $K_v1.5$-CFP expression (Fig. 5*D*).

Ventricular KCNE4 expression is regulated by DHT

Electrocardiographic analyses showed that, in 4-mo-old male mice, QT_c, a measure of the time for ventricular repolarization, was unaltered by *Kcne4* deletion. In contrast,

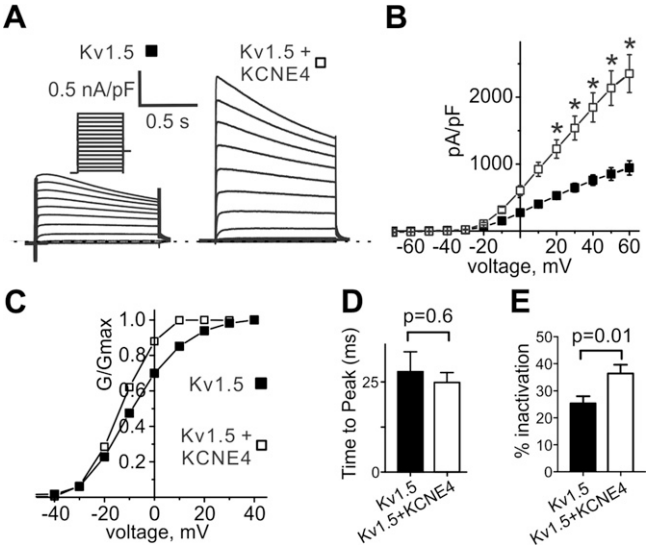

Figure 4. KCNE4 doubles $K_v1.5$ current density in CHO cells. *A*) Representative whole-cell K^+ current traces recorded from CHO cells 48 h after transfection of $K_v1.5$ alone or with KCNE4 (voltage protocol inset); n = 20–21. *B*) Mean peak current density for cells as in *A*; n = 20–21, $^*P < 0.0001$. *C–E*) Mean voltage dependence of activation (*C*), time to peak activation (*D*), and percent inactivation (*E*) for currents as in *A* and *B*; n values as in *A* and *B*.

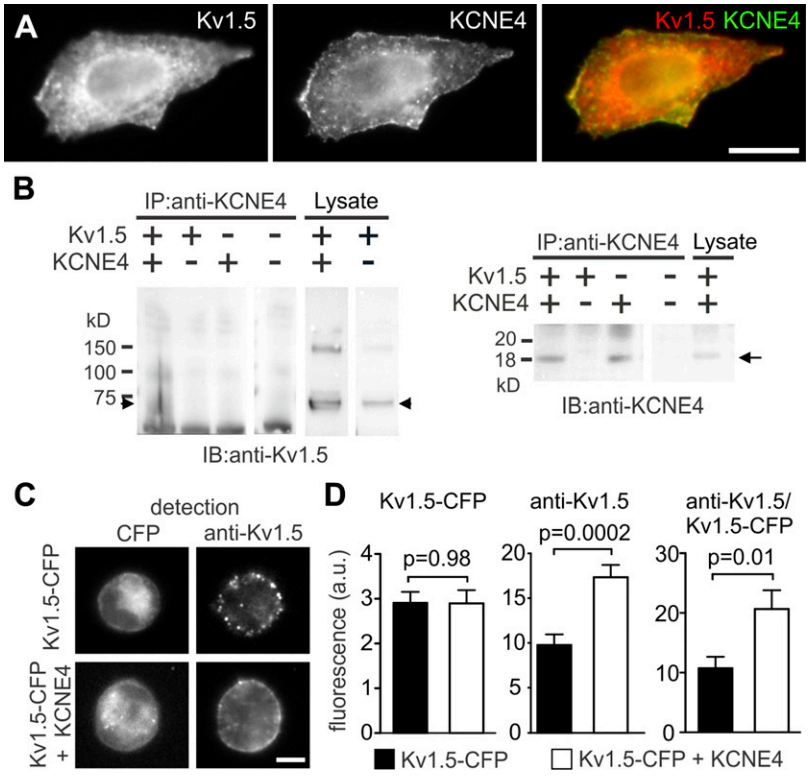

Figure 5. KCNE4 forms complexes with, and doubles surface expression of, $K_v1.5$ in CHO cells. *A*) Fluorescence micrographs showing plasma membrane colocalization of KCNE4 and $K_v1.5$, taken 48 h after transfection of CHO cells. Scale bar, 2.5 μm. *B*) Left) Coimmunoprecipitation (IP) of $K_v1.5$ and KCNE4 from lysates isolated 48 h after CHO cell transfection. Proteins were immunoprecipitated with anti-KCNE4 antibody and immunoblotted (IB) using anti-$K_v1.5$ antibody. Arrow, $K_v1.5$ monomer. Lysate, lanes loaded with nonimmunoprecipitated lysate for control. cDNAs transfected are indicated by + and their absence by −. Right) Positive control for KCNE4 IP and IB, both using KCNE4 antibody. Arrow, KCNE4 monomer; other symbols as in upper blot. *C*) Fluorescence micrographs of live CHO cells expressing CFP-tagged $K_v1.5$ alone or with KCNE4. Fluorescence signal detected was either CFP (left) to quantify total $K_v1.5$-CFP expression or *via* antibody raised to an external epitope on $K_v1.5$ (right) to quantify $K_v1.5$-CFP surface expression, in the same cell. Scale bar, 2.5 μm. *D*) Quantification of mean effects of KCNE4 on total (left), surface (center), and surface/total (right) $K_v1.5$ expression; n = 22–23 cells per group.

Kcne4 deletion increased QT_c by 24% at 12 mo of age and by 55% at 17 mo of age in male mice (**Fig. 6*A***). This pattern was not entirely unexpected: we observed similar age-dependent *Kcne*-dependent QTc prolongation in both the *Kcne2*$^{-/-}$ and *Kcne3*$^{-/-}$ mouse lines (27, 28), suggesting that *Kcne2, 3,* or *4* deletion requires additional aging-related erosion of the repolarization reserve to manifest on the body surface electrocardiogram.

We also observed aging-dependent QT_c prolongation in female *Kcne4*$^{-/-}$ mice, except that it occurred with a later onset than in males. Thus, QT_c of female mice was unaltered by *Kcne4* deletion at 4 and 12 mo but increased by 47% at 17 mo (Fig. 6*B*), by which age female mice are postmenopausal (29). That *Kcne4* deletion had an effect on postmenopausal female QT_c was surprising, given the relatively low cardiac expression of KCNE4 in young adult female mice (Fig. 1*B*). Other electrocardiographic parameters were not changed in either sex (Supplemental Fig. S2). Similarly, hemodynamic parameters were largely unaffected by *Kcne4* deletion (Supplemental Fig. S3). Mean minimum change in pressure/time (Min dP/dt) was high in female *Kcne4*$^{-/-}$ mice compared with *Kcne4*$^{+/+}$ mice (n = 7–8; P = 0.028), but the possible implications of this will require future investigation.

Given the unexpected importance of the Kcne4 subunit in ventricular repolarization of postmenopausal female mice, we quantified their *Kcne4* expression and found that ventricular *Kcne4* expression was >10-fold higher in

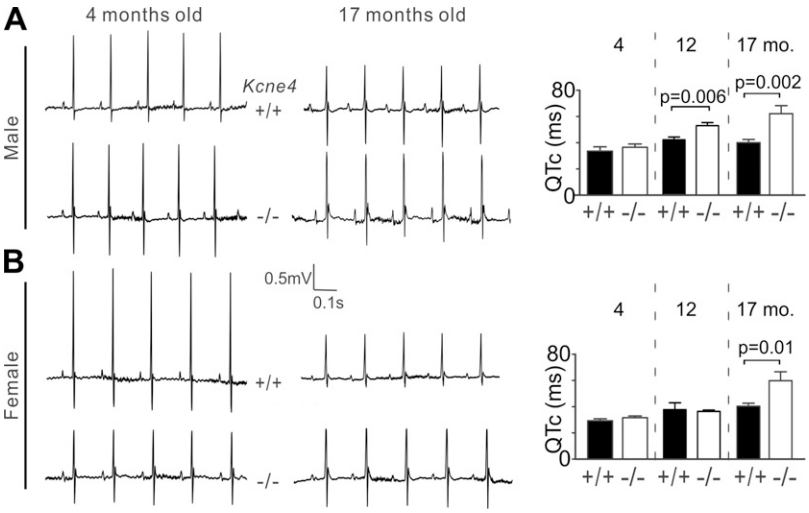

Figure 6. Effects of Kcne4 deletion on ventricular repolarization are age and sex dependent. *A*) Left) Representative body surface electrocardiograms measured from 4- (n = 11) and 17-mo-old (n = 8–10) male *Kcne4*$^{+/+}$ and *Kcne4*$^{-/-}$ mice as indicated. Right) Mean QT_c values quantified from electrocardiograms as in left and from 12-mo-old male mice (n = 5–8). *B*) Left) Representative body surface electrocardiograms measured from 4- (n = 9–10) and 17-mo-old (n = 10–12) female *Kcne4*$^{+/+}$ and *Kcne4*$^{-/-}$ mice as indicated. Right) Mean QTc values quantified from electrocardiograms as in left and from 12-mo-old female mice (n = 3).

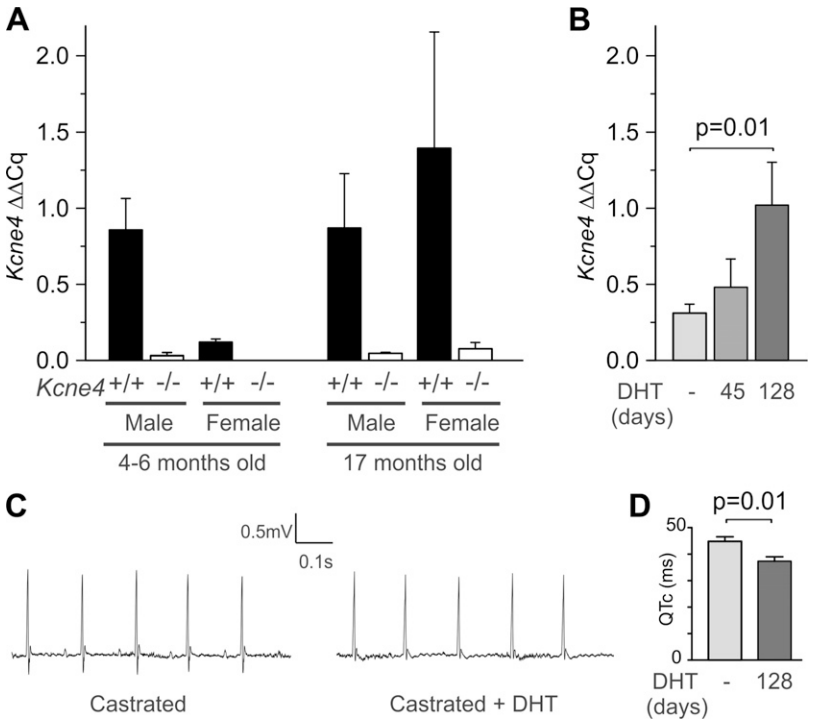

Figure 7. DHT regulates ventricular *Kcne4* expression and ventricular repolarization. *A*) Real-time qPCR quantification of *Kcne4* expression in 4- and 17-mo-old mouse heart left ventricles. *Kcne4*$^{-/-}$ tissue (open columns) was used as a negative control. *Kcne4* expression levels for young adult male and female left ventricles are repeated from Fig. 1*D* for comparison. All values were normalized to one of the 4- to 6-mo-old male *Kcne4*$^{+/+}$ mouse *Kcne4* expression values. *B*) Real-time qPCR quantification of *Kcne4* expression in left ventricles from castrated mice (light gray, $n = 9$), and castrated/DHT pellet-implanted young adult male mice 45 (medium gray, $n = 5$) and 128 d (dark gray, $n = 4$) after implant, each quantified in triplicate. *Kcne4* expression in nonpellet-implanted *vs.* 128 d after pellet implant, $P = 0.01$; all other comparisons, $P > 0.05$, by Tukey honest significant difference, Scheffé multiple comparison, or Bonferroni and Holm multiple comparison. All values were normalized to one of the 4- to 6-mo-old male *Kcne4*$^{+/+}$ mouse *Kcne4* expression values from *A*. *C*) Representative body surface electrocardiograms measured from 6-mo-old castrated ($n = 5$) and castrated, DHT pellet-implanted (128 d) male *Kcne4*$^{+/+}$ mice as indicated. *D*) Mean QT_c values quantified from electrocardiograms as in *C* ($n = 5$).

postmenopausal female mice compared with young sexually mature (4–6 mo old) adult female mice and was equivalent to that of young and old adult male mice (**Fig. 7*A***).

Interestingly, in young adult mice, DHT is very high in males compared with females (a ratio of >50:1), but DHT levels rise >4-fold after menopause in female mice (29), qualitatively matching the pattern we observed for the *Kcne4* transcript. To test the hypothesis that DHT regulates ventricular *Kcne4* expression, we quantified the latter in young adult male mice that had been castrated at 2 mo of age and those that were castrated and simultaneously implanted with DHT pellets. At 128 d after pellet implantation, left ventricular *Kcne4* expression was >3-fold higher than that of castrated, nonpellet-implanted mice ($P = 0.01$) and similar to that of noncastrated male mice (Fig. 7*A, B*). *Kcne4* expression 45 d after pellet implantation was intermediate between that of castrated, nonpellet-implanted and castrated mice 128 d after DHT pellet implant (Fig. 7*B*). Consistent with the DHT-dependent expression of *Kcne4* and the observation that *Kcne4* deletion prolongs the QT interval by diminishing ventricular K_v currents generated by channels regulated by Kcne4, DHT pellet implantation shortened the QT_c interval in castrated mice (Fig. 7*C, D*).

DISCUSSION

Our findings reveal that DHT positively regulates *Kcne4* expression in mouse ventricles and that this contributes to higher K_v current density in young adult male mice compared with their age-matched female counterparts. Postmenopausal female mice exhibit an increase in ventricular *Kcne4* expression concomitant with the increased DHT known to occur on this transition (29). Interestingly, in a previous study, ventricular myocyte $I_{K,slow}$ density was found to be higher in male mice than in females, with the difference linked to DHT regulation of $K_v1.5$ (30). In that study, as we recapitulated here (Fig. 7*C, D*), DHT shortened the QT_c in castrated mice. Our findings suggest that control of QT_c by DHT arises from its positive regulation not just of $K_v1.5$ but also of KCNE4. Also in the prior study (30), it was found that C57BL/6 male mice have relatively low DHT compared with another strain, CD-1, and that males of the latter strain also exhibit higher 4-AP–sensitive current density than do C57BL/6 male mice. It is possible that a backcross of our *Kcne4*$^{-/-}$ mice into the CD-1 background would yield even larger differences in *Kcne4* expression between sexes than seen here.

Our data are the first to demonstrate male androgen regulation of a K^+ channel regulatory subunit, although estrogen (and not DHT) was previously shown to positively regulate Kcne2 expression in the murine heart (31). It was suggested that such regulation provides a mechanism to counteract other factors causing QT prolongation by reducing the repolarization reserve near the end of gestation, with the surge in estrogen during this period upregulating Kcne2, which could augment $I_{to,f}$ and $I_{K,slow1}$, based on our previous findings (7). Similarly, DHT upregulation of Kcne4 expression might provide a mechanism for augmenting $I_{to,f}$ and $I_{K,slow1}$ in postmenopausal female mice to counteract the QT-prolonging effects of aging that we have now observed in 3 separate *Kcne*$^{-/-}$ mouse colonies (27, 28).

It therefore appears that Kcne2 and Kcne4 serve, in some ways, similar roles in mouse ventricles, each augmenting both I_{to} and $I_{Kslow,1}$, Kcne2 being relatively more

prominent in the female heart because of positive regulation by estrogen and Kcne4 more important in males because of positive regulation by DHT. Both Kcne2 and Kcne4 are expressed in multiple tissues outside the heart (32), yet hormonal regulation of these subunits in other tissues has not been studied. To fully understand the ramifications of this mode of regulation, a more comprehensive analysis is warranted. In addition, we do not yet know the mechanism by which DHT regulates *Kcne4* expression. Typically, DHT binds to androgen receptors, and the complex translocates to the nucleus, where it binds to androgen-responsive elements (AREs) on specific genes. We did not find a canonical ARE within the mouse *Kcne4* gene sequence, suggesting either *Kcne4* harbors a noncanonical ARE or DHT increases *Kcne4* expression by activating another protein (*e.g.*, another transcription factor). DHT can also act nongenomically (*e.g.*, its binding to androgen receptors can rapidly activate mitogen-activated protein kinases), resulting in downstream activation of transcription factors (33)—another avenue to explore in future directions.

It is possible that Kcne4 is upregulated by DHT to mirror DHT up-regulation of $K_v1.5$ similar to the coordinated expression of K_v4 and KChIP subunits in mice (34), presumably to avoid the deleterious effects of expression of $K_v1.5$ without the modifications produced by Kcne4 on channel function and trafficking that might result from an expression level mismatch. The same might apply to $K_v4.2$ and/or $K_v4.3$, the subunits generating $I_{to,f}$ in mouse ventricles. $K_v4.3$ was previously found to be upregulated by testosterone in female canine ventricles and more highly expressed in normal male than in normal female ventricles (35).

Turning to the atria, we found that *Kcne4* deletion primarily affected $I_{to,f}$, reducing current density by more than half, although we did not detect spontaneous atrial arrhythmias in *Kcne4*$^{-/-}$ mice. The 36% reduction in $I_{K,slow}$ density did not reach the $P < 0.05$ significance level, but was comparable to the effect we observed for ventricular $I_{K,slow}$ of male *Kcne4*$^{-/-}$ mice. In human heart, KCNE4 expression is reported to be 2-fold higher in the atria over the ventricles (36); this may explain the link between KCNE4 and AF (19–21), whereas ventricular arrhythmias have not been reported to date. Interestingly, unlike in the adult murine heart, $K_v1.5$ in the human heart is enriched in the atria compared with the ventricles (where it is difficult to detect) (37). Prior studies of the human *KCNE4* G/T polymorphism at position 1057 found that the T allele (generating the KCNE4 145D *vs.* 145E for the G allele) is associated with increased incidence of AF (19–21). *In vitro* studies showed that KCNE4-145D augmented KCNQ1 current, whereas 145E inhibited it, a plausible mechanism for AF (22). In light of our findings, it will be of interest to compare the effects of the 2 human KCNE4 variants on $K_v1.5$ and $K_v4.2/3$ channel properties to determine whether these potentially contribute to, or counteract, effects on KCNQ1.

Finally, further studies are required to determine whether KCNE4 and KCNE2 are also regulated by hormones in human heart. AF is much more common in the elderly than in the young and afflicts millions within the aging population in the United States alone. As testosterone levels diminish later in life in men, it will be important to determine how the predicted reduction in cardiac *KCNE4* associated with this might affect susceptibility to AF and to consider the potential safety and efficacy of correcting this with hormonal therapy. In a recent analysis of the Framingham Heart Study, testosterone deficiency in men of 80 yr of age and older was found to be strongly associated with AF risk, whereas the mechanistic basis remains incompletely understood (38). The results of mouse studies cannot be directly extrapolated to the human heart because of major differences in, for example, heart rate, chamber size, and K_v channel subunit expression. However, the more we understand about these differences, the more effectively we can use studies of the genetically highly tractable mouse to generate testable hypotheses relating to crucial aspects of human cardiac physiology and the pathogenesis of debilitating or lethal cardiac arrhythmias. FJ

The authors thank Daniel Neverisky and Soo Min Lee (University of California, Irvine) for expert technical assistance. This work was funded by U.S. National Institutes of Health National Heart, Lung and Blood Institute (NHLBI) Grants HL079275 (to G.W.A.) and HL105949 (to S.A.N.G.). S.M.C. was supported by NHLBI Postdoctoral Diversity Supplement HL079275-S1 (to G.W.A.).

REFERENCES

1. Abbott, G. W. (2006) Molecular mechanisms of cardiac voltage-gated potassium channelopathies. *Curr. Pharm. Des.* **12**, 3631–3644
2. Abbott, G. W., and Goldstein, S. A. (1998) A superfamily of small potassium channel subunits: form and function of the MinK-related peptides (MiRPs). *Q. Rev. Biophys.* **31**, 357–398
3. Abbott, G. W. (2014) Biology of the KCNQ1 potassium channel. *New J. Sci.* **2014**, 1–26
4. Nerbonne, J. M., Nichols, C. G., Schwarz, T. L., and Escande, D. (2001) Genetic manipulation of cardiac K(+) channel function in mice: what have we learned, and where do we go from here? *Circ. Res.* **89**, 944–956
5. Kanda, V. A., and Abbott, G. W. (2012) KCNE regulation of K(+) channel trafficking: a sisyphean task? *Front. Physiol.* **3**, 231
6. Abbott, G. W., Sesti, F., Splawski, I., Buck, M. E., Lehmann, M. H., Timothy, K. W., Keating, M. T., and Goldstein, S. A. (1999) MiRP1 forms IKr potassium channels with HERG and is associated with cardiac arrhythmia. *Cell* **97**, 175–187
7. Roepke, T. K., Kontogeorgis, A., Ovanez, C., Xu, X., Young, J. B., Purtell, K., Goldstein, P. A., Christini, D. J., Peters, N. S., Akar, F. G., Gutstein, D. E., Lerner, D. J., and Abbott, G. W. (2008) Targeted deletion of kcne2 impairs ventricular repolarization via disruption of I(K,slow1) and I(to,f). *FASEB J.* **22**, 3648–3660
8. Crump, S. M., and Abbott, G. W. (2014) Arrhythmogenic KCNE gene variants: current knowledge and future challenges. *Front. Genet.* **5**, 3
9. Yang, P. C., and Clancy, C. E. (2010) Effects of sex hormones on cardiac repolarization. *J. Cardiovasc. Pharmacol.* **56**, 123–129
10. Wilde, A. A., Antzelevitch, C., Borggrefe, M., Brugada, J., Brugada, R., Brugada, P., Corrado, D., Hauer, R. N., Kass, R. S., Nademanee, K., Priori, S. G., and Towbin, J. A.; Study Group on the Molecular Basis of Arrhythmias of the European Society of Cardiology (2002) Proposed diagnostic criteria for the Brugada syndrome: consensus report. *Circulation* **106**, 2514–2519
11. Kurokawa, J., Kodama, M., Furukawa, T., and Clancy, C. E. (2012) Sex and gender aspects in antiarrhythmic therapy. *Handbook Exp. Pharmacol.* 214, 237–263
12. Grunnet, M., Jespersen, T., Rasmussen, H. B., Ljungstrøm, T., Jorgensen, N. K., Olesen, S. P., and Klaerke, D. A. (2002) KCNE4 is an inhibitory subunit to the KCNQ1 channel. *J. Physiol.* **542**, 119–130
13. Grunnet, M., Olesen, S. P., Klaerke, D. A., and Jespersen, T. (2005) hKCNE4 inhibits the hKCNQ1 potassium current without affecting the activation kinetics. *Biochem. Biophys. Res. Commun.* **328**, 1146–1153

14. Grunnet, M., Rasmussen, H. B., Hay-Schmidt, A., Rosenstierne, M., Klaerke, D. A., Olesen, S. P., and Jespersen, T. (2003) KCNE4 is an inhibitory subunit to Kv1.1 and Kv1.3 potassium channels. *Biophys. J.* **85**, 1525–1537
15. Radicke, S., Cotella, D., Graf, E. M., Banse, U., Jost, N., Varró, A., Tseng, G. N., Ravens, U., and Wettwer, E. (2006) Functional modulation of the transient outward current Ito by KCNE beta-subunits and regional distribution in human non-failing and failing hearts. *Cardiovasc. Res.* **71**, 695–703
16. Solé, L., Roura-Ferrer, M., Pérez-Verdaguer, M., Oliveras, A., Calvo, M., Fernández-Fernández, J. M., and Felipe, A. (2009) KCNE4 suppresses Kv1.3 currents by modulating trafficking, surface expression and channel gating. *J. Cell Sci.* **122**, 3738–3748
17. Levy, D. I., Cepaitis, E., Wanderling, S., Toth, P. T., Archer, S. L., and Goldstein, S. A. (2010) The membrane protein MiRP3 regulates Kv4. 2 channels in a KChIP-dependent manner. *J. Physiol.* **588**, 2657–2668
18. Levy, D. I., Wanderling, S., Biemesderfer, D., and Goldstein, S. A. (2008) MiRP3 acts as an accessory subunit with the BK potassium channel. *Am. J. Physiol. Renal Physiol.* **295**, F380–F387
19. Zeng, Z., Tan, C., Teng, S., Chen, J., Su, S., Zhou, X., Wang, F., Zhang, S., Gu, D., Makielski, J. C., and Pu, J. (2007) The single nucleotide polymorphisms of I(Ks) potassium channel genes and their association with atrial fibrillation in a Chinese population. *Cardiology* **108**, 97–103
20. Zeng, Z. Y., Pu, J. L., Tan, C., Teng, S. Y., Chen, J. H., Su, S. Y., Zhou, X. Y., Zhang, S., Li, Y. S., Wang, F. Z., and Gu, D. F. (2005) [The association of single nucleotide polymorphism of slow delayed rectifier K+ channel genes with atrial fibrillation in Han nationality Chinese]. *Zhonghua Xin Xue Guan Bing Za Zhi* **33**, 987–991
21. Mao, T., Miao, H. J., Xu, G. J., Gan, T. Y., Zhou, X. H., Zhang, J., Li, F. P., and Tang, B. P. (2013) [Association of single nucleotide polymorphism of KCNE1 and KCNE4 gene with atrial fibrillation in Xinjiang Uygur and Han population]. *Zhonghua Xin Xue Guan Bing Za Zhi* **41**, 916–921
22. Ma, K. J., Li, N., Teng, S. Y., Zhang, Y. H., Sun, Q., Gu, D. F., and Pu, J. L. (2007) Modulation of KCNQ1 current by atrial fibrillation-associated KCNE4 (145E/D) gene polymorphism. *Chin. Med. J. (Engl.)* **120**, 150–154
23. Kanda, V. A., Lewis, A., Xu, X., and Abbott, G. W. (2011) KCNE1 and KCNE2 inhibit forward trafficking of homomeric N-type voltage-gated potassium channels. *Biophys. J.* **101**, 1354–1363
24. Mitchell, G. F., Jeron, A., and Koren, G. (1998) Measurement of heart rate and Q-T interval in the conscious mouse. *Am. J. Physiol.* **274**, H747–H751
25. Xu, H., Guo, W., and Nerbonne, J. M. (1999) Four kinetically distinct depolarization-activated K+ currents in adult mouse ventricular myocytes. *J. Gen. Physiol.* **113**, 661–678
26. Bou-Abboud, E., Li, H., and Nerbonne, J. M. (2000) Molecular diversity of the repolarizing voltage-gated K+ currents in mouse atrial cells. *J. Physiol.* **529**, 345–358
27. Hu, Z., Crump, S. M., Anand, M., Kant, R., Levi, R., and Abbott, G. W. (2014) Kcne3 deletion initiates extracardiac arrhythmogenesis in mice. *FASEB J.* **28**, 935–945
28. Hu, Z., Kant, R., Anand, M., King, E. C., Krogh-Madsen, T., Christini, D. J., and Abbott, G. W. (2014) Kcne2 deletion creates a multisystem syndrome predisposing to sudden cardiac death. *Circ. Cardiovasc. Genet.* **7**, 33–42
29. Nilsson, M. E., Vandenput, L., Tivesten, Å., Norlén, A. K., Lagerquist, M. K., Windahl, S. H., Börjesson, A. E., Farman, H. H., Poutanen, M., Benrick, A., Maliqueo, M., Stener-Victorin, E., Ryberg, H., and Ohlsson, C. (2015) Measurement of a comprehensive sex steroid profile in rodent serum by high-sensitive gas chromatography-tandem mass spectrometry. *Endocrinology* **156**, 2492–2502
30. Brouillette, J., Rivard, K., Lizotte, E., and Fiset, C. (2005) Sex and strain differences in adult mouse cardiac repolarization: importance of androgens. *Cardiovasc. Res.* **65**, 148–157
31. Kundu, P., Ciobotaru, A., Foroughi, S., Toro, L., Stefani, E., and Eghbali, M. (2008) Hormonal regulation of cardiac KCNE2 gene expression. *Mol. Cell. Endocrinol.* **292**, 50–62
32. McCrossan, Z. A., and Abbott, G. W. (2004) The MinK-related peptides. *Neuropharmacology* **47**, 787–821
33. Peterziel, H., Mink, S., Schonert, A., Becker, M., Klocker, H., and Cato, A. C. (1999) Rapid signalling by androgen receptor in prostate cancer cells. *Oncogene* **18**, 6322–6329
34. Foeger, N. C., Wang, W., Mellor, R. L., and Nerbonne, J. M. (2013) Stabilization of Kv4 protein by the accessory K(+) channel interacting protein 2 (KChIP2) subunit is required for the generation of native myocardial fast transient outward K(+) currents. *J. Physiol.* **591**, 4149–4166
35. Fülöp, L., Bányász, T., Szabó, G., Tóth, I. B., Bíró, T., Lôrincz, I., Balogh, A., Petô, K., Mikó, I., and Nánási, P. P. (2006) Effects of sex hormones on ECG parameters and expression of cardiac ion channels in dogs. *Acta Physiol. (Oxf.)* **188**, 163–171
36. Bendahhou, S., Marionneau, C., Haurogne, K., Larroque, M. M., Derand, R., Szuts, V., Escande, D., Demolombe, S., and Barhanin, J. (2005) In vitro molecular interactions and distribution of KCNE family with KCNQ1 in the human heart. *Cardiovasc. Res.* **67**, 529–538
37. Gaborit, N., Le Bouter, S., Szuts, V., Varro, A., Escande, D., Nattel, S., and Demolombe, S. (2007) Regional and tissue specific transcript signatures of ion channel genes in the non-diseased human heart. *J. Physiol.* **582**, 675–693
38. Magnani, J. W., Moser, C. B., Murabito, J. M., Sullivan, L. M., Wang, N., Ellinor, P. T., Vasan, R. S., Benjamin, E. J., and Coviello, A. D. (2014) Association of sex hormones, aging, and atrial fibrillation in men: the Framingham Heart Study. *Circ. Arrhythm. Electrophysiol.* **7**, 307–312

Received for publication July 8, 2015.
Accepted for publication September 8, 2015.